Propofol alleviates M1 polarization and neuroinflammation of microglia in a subarachnoid hemorrhage model *in vitro*, by targeting the miR-140-5p/TREM-1/NF-κB signaling axis

Lan Wang,[1#] Zhenyu Fan,[1#] Haijin Wang,[1] Shougui Xiang[2]

[1]Department of Anesthesiology
[2]Department of Critical Care Medicine, Xiangyang No.1 People's Hospital, Hubei University of Medicine, Xiangyang, China

[#]These authors contributed equally to this work.

ABSTRACT

Subarachnoid hemorrhage (SAH) is a devastating stroke caused by ruptured intracranial aneurysms, leading to blood accumulation around the brain. Early brain injury (EBI) within 72 h post-SAH worsens prognosis, primarily due to intense neuroinflammation. Microglia, pivotal in central nervous system defense and repair, undergo M1 to M2 polarization post-SAH, with M1 exacerbating neuroinflammation. Propofol (PPF), an anesthetic with anti-inflammatory properties, shows promise in mitigating neuroinflammation in SAH by modulating microglial activation. It likely acts through microRNAs like miR-140-5p, which attenuates microglial activation and inflammation by targeting TREM-1 and the NF-κB pathway. Understanding these mechanisms could lead to new therapeutic approaches for SAH-related EBI. In this study, BV-2 cell was used to establish *in vitro* model of SAH, and the expression of miR-140-5p and TREM-1 was detected after modeling. Microglial activity, apoptosis, the inflammatory pathway and response, oxidative damage, and M1/M2 polarization of microglia were evaluated by drug administration or transfection according to experimental groups. Finally, the targeting relationship between miR-140-5p and TREM-1 was verified by dual luciferase reporter assays, and the effect of PPF on the miR-140-5p/TREM-1/NF-κB signaling cascade was evaluated by RT–qPCR or Western blotting. PPF effectively mitigates apoptosis, neuroinflammation, oxidative damage, and M1 microglial polarization in SAH. In SAH cells, PPF upregulates miR-140-5p and downregulates TREM-1. Mechanistically, PPF boosts miR-140-5p expression, while TREM-1, a downstream target of miR-140-5p, inhibits NF-κB signaling by regulating TREM-1, promoting M1 to M2 microglial polarization. Reduced miR-140-5p or increased TREM-1 counters PPF's therapeutic impact on SAH cells. In conclusion, PPF plays a neuroprotective role in SAH by regulating the miR-140-5p/TREM-1/NF-κB signaling axis to inhibit neuroinflammation and M1 polarization of microglia.

Key words: subarachnoid hemorrhage; propofol; miR-140-5p; TREM-1; microglia; M1 polarization.

Correspondence: Dr. Shougui Xiang, Department of Critical Care Medicine, Xiangyang No. 1 People's Hospital, Hubei University of Medicine, 15 Jiefang Road, Fancheng District, Xiangyang, Hubei 441000, China.
E-mail: Xiangshougui_HBMU@163.com

Contributions: all the authors made a substantive intellectual contribution, read and approved the final version of the manuscript and agreed to be accountable for all aspects of the work.

Conflict of interest: the authors declare that they have no competing interests, and all authors confirm accuracy.

Ethics approval: not applicable.

Introduction

Subarachnoid hemorrhage (SAH), mainly caused by a ruptured aneurysm, is a devastating hemorrhagic stroke with high mortality that is characterized by blood accumulation in the subarachnoid space surrounding the brain.[1] The latest evidence shows that early brain injury (EBI) occurring within 72 h after SAH is a key factor leading to poor prognosis in SAH patients.[2,3] Among them, intense neuroinflammation after SAH is considered to be a key factor in the progression of EBI after SAH.[4] As an important mediator of neuroinflammation, microglia play a key role in host defense and tissue repair in the central nervous system and are rapidly activated after various acute brain injuries (including SAH).[5] In SAH, many studies have reported that M1 microglia predominate in the beginning and then transition to the M2 phenotype. Inhibiting M1 polarization of microglia can significantly improve neuroinflammation and nervous system outcomes after SAH.[6] It is also noteworthy to consider the interactions of microglia with astroglia, another essential glial cell type in neuroinflammation. Astroglia, through their close communication with microglial cells, further regulate inflammatory responses and contribute significantly to the overall neuroinflammatory environment in SAH and other brain injuries. These effects might be mediated by microRNAs (miRNAs). Certain dysregulated miRNAs may lead to chronic microglial inflammation, which in turn leads to the development of neurodegenerative diseases.[7] Therefore, therapeutic strategies targeting the transformation of microglia can be used as an entry point to reverse the progression of EBI after SAH. Experiments can be carried out to further explore the pathological progression of SAH and enrich therapeutic strategies for SAH. Propofol (2,6-diisopropyl phenol, PPF) is a widely used short-acting intravenous anesthetic that is often used in the clinical treatment of analgesia and as an anticonvulsant. In addition to hypnosis and sedation, PPF also has anti-inflammatory properties, which can reduce the production of pro-inflammatory cytokines, change the expression of nitric oxide, and inhibit the function of neutrophils.[8] There is evidence that PPF can reduce microglial activation when cells are exposed to external stimuli.[9,10] In addition, in the latest preclinical studies, PPF has been shown to reduce inflammatory brain injury after SAH and has neuroprotective effects.[11,12] However, the effect of PPF on EBI-associated microglial activation after SAH remains largely unknown. In addition, the molecular mechanism by which PPF confers anti-inflammatory activity in microglia remains to be elucidated. As small noncoding RNAs, miRNAs have been comprehensively studied for their important regulatory functions in microglial activation. We noted that several previous studies have shown that PPF reduces microglial activation and the inflammatory response by regulating miRNA expression.[10,13] Therefore, we speculated that PPF regulates the progression of EBI after the phenotypic transformation of microglia reverses SAH, and its mechanism of action may be related to downstream miRNAs.

MicroRNA-140-5p (miR-140-5p) is a well-known inflammation-associated miRNA that regulates inflammation, anti-apoptosis, and immune responses in many human diseases. Studies have confirmed that miR-140-5p is involved in nerve damage in various cerebrovascular diseases.[14,15] Importantly, recent preclinical studies have manifested that miR-140-5p weakens SAH-induced microglial activation and the inflammatory response, as well as neuronal damage, mainly by regulating downstream pathways.[16,17] In addition, PPF can play a therapeutic role in other diseases by upregulating miR-140-5p.[18] Therefore, miR-140-5p was the most popular candidate gene in our study. Subsequently, a bioinformatics prediction website showed that trigger receptor 1 (TREM-1) expressed on myeloid cells could be used as the downstream target gene of miR-140-5p. Elevated TREM-1 has been shown to be associated with poor prognosis in patients with SAH.[19,20] In addition, TREM-1 can participate in the activation of the nuclear factor-κB (NF-κB) signaling cascade by coupling with DAP-12.[21] Recent studies have shown that restriction of the NF-κB cascade can contribute to relieve EBI after SAH.[22] More importantly, activation of the NF-κB cascade is associated with an increase in aneurysm microglial cell populations.[23] Based on the above background, we hypothesized that PPF ameliorates SAH neuroinflammation by regulating the miR-140-5p/TREM-1/NF-κB signaling axis to mediate microglial phenotypic transformation. In this study, the effects of PPF on M1/M2 polarization and neuroinflammatory damage in microglia induced by EBI after SAH were studied using an SAH cell model and microglial phenotypic transformation as an entry point. On this basis, the influence of PPF on EBI after SAH mediated by the miR-140-5p/TREM-1/NF-κB signaling axis and its possible regulatory mechanism were further discussed.

Materials and Methods

Cellular Model

BV-2 microglia were used (National Cell Line Resource Infrastructure). The cells were cultured in DMEM (C11995500BT; Gibco, Rockville, MD, USA) containing 10% FBS and 1% penicillin/streptomycin at 37°C and 5% CO2. Oxygenated hemoglobin (OxyHb, 25 μM) was added to BV-2 cells for 24 h to establish an *in vitro* SAH model.[24] BV-2 cells were treated with 100 nM rapamycin (R485503, Aladdin Scientific, Washington DC, WA, USA) and 1 mM DMOG (D408454; Aladdin Scientific) for 1 h before OxyHb induction.

Experimental grouping and administration

Cells in the logarithmic growth stage were selected for experimental intervention and grouping and randomly divided into 13 groups, as shown in Table 1. For PPF (Aladdin Scientific) treatment, BV-2 microglia were incubated with different concentrations of PPF (0, 6.25, 12.5, 25, 50 and 100 μM) for 24 h after OxyHb induction, and the optimal administration concentration of PPF was selected according to cell activity and used as the experimental concentration for the following experiments. miR-140-5p mimic or inhibitors (miR-140-5p mimic/in-miR-140-5p), overexpression plasmids targeting TREM-1 (OE-TREM-1) or short hairpin RNA (sh-TREM-1) and their negative controls (sh-NC, OE-NC, mimic NC, in-NC) were all purchased from RiboBio Co. Ltd. (Guangzhou, China). When the cells adhered to the wall and reached approximately 80% confluence, the above plasmids and RNA were transfected into BV-2 cells using Lipofectamine 3000 reagent according to the manufacturer's instructions. The transfection efficiency was verified by RT–qPCR. The follow-up experiment was carried out 24 h after the experimental intervention.

CCK-8

Cell viability was assessed by a CCK-8 Cell Counting Kit (C0038; Beyotime, Shanghai, China). Logarithmic cells were inoculated in 96-well plates, and 10 μL of CCK-8 solution was added to each well for 2 h. Optical density (OD) values were measured at 450 nm with an enzyme marker.

Flow cytometry (FCM)

BV-2 cells were inoculated into a 6-well plate (5×10^5 cells/well) for SAH stimulation and transfection as described above. This was followed by reaction with 5 μL Annexin V-FITC and 10 μL PI (40302ES20; Yeasen, Shanghai, China) in the dark for 5 min. Finally, apoptotic cells were counted by an Attune™

NxT Flow Cytometer (A24858; Invitrogen, Carlsbad, CA, USA).

The percentage of the M1/M2 microglial phenotype was determined by assessing the levels of CD86 and CD206, the corresponding markers of the M1/M2 microglial phenotype. BV-2 cells were collected and adjusted to 2×10^6 cells/well after digestion by pancreatic enzymes. When the degree of cell fusion was approximately 80%, the cells were digested, resuspended and counted. Fifty microliters of single-cell suspension (approximately 1×10^6 cells) was added to 10 μL of CD86 (AF1447; Beyotime, Shanghai, China) and CD206 (AG2660; Beyotime) antibodies with fluorescent marker FITC-labeled Goat Anti-Rabbit IgG(H+L) (A0562; Beyotime) and incubated at room temperature for 60 min away from light. Finally, the percentages of CD86 and CD206 were measured in an Attune™ NxT Flow Cytometer (A24858; Invitrogen) equipped with FlowJo software.

ELISA

The BV-2 cell culture supernatant was collected following the manufacturer's instructions. Cytokine concentrations were measured by an IL-1β ELISA kit (KE10003; Proteintech, Rosemont, IL, USA), TNF-α ELISA kit (KE10002; Proteintech), and IL-6 ELISA kit (KE10008; Proteintech).

Oxidative stress reaction analysis

The BV-2 cells were collected and dissolved in 0.2% Triton X-100 (100-100 ML; Sigma-Aldrich, St. Louis, MO, USA). After centrifugation, 50 μL of supernatant was collected for the experiment. The SOD Assay Kit (S0101S; Beyotime) or MDA Assay Kit (S0131S; Beyotime) was applied to detect the activity levels of superoxide dismutase (SOD) and malondialdehyde (MDA) according to the manufacturer's instructions. Similarly, an ROS assay kit (S0033S; Beyotime) was used to assess the production of reactive oxygen species (ROS).

RT-qPCR

RNA extraction was carried out using a TRIzol kit (RC112-01; Vazyme, Nanjing, China), and the concentration of RNA was determined. HiScript lll 1st Strand cDNA Synthesis Kit (R211-02; Vazyme) for reverse transcription; Taq Pro Universal SYBR qPCR Master Mix (Q712-02; Vazyme) was applied to real-time PCR with the following cycle conditions: 95°C 5 min (predenaturation), 95°C 10 s (denaturation), 60°C 1 min (annealing/extension), 40 cycles. U6 and GAPDH were used to normalize miR-140-5p and mRNA, respectively. The primers are shown in Table 2.

Western blot

Protein was extracted from cell precipitation by radioimmunoprecipitation (RIPA, BL504A, Biosharp, Hefei, China) buffer containing protease inhibitors. An equal amount of protein was added to each sample, separated by SDS-PAGE (Criterion™ Cell; Bio-Rad, Hercules, CA, USA), and then transferred to a PVDF membrane for separation. Subsequently, the membrane was closed with 5% skim milk at room temperature for 2 h, and then incubated with primary antibody at 4°C overnight. Then, the membrane was incubated with the secondary antibody (1:10,000, bs-0295G-HRP) for 2 h. The imprinted tape was visualized and exposed to X-ray film using enhanced chemiluminescence (ECL, NCM Biotech, Suzhou, China), and ImageJ software was used for analysis. The primary antibodies used are as follows: Rabbit Anti-TREM-1 antibody (1:1000, TA-08, ZSBG-Bio), Rabbit Anti-pNF-κB antibody (1:1000, TA-08, ZSBG-Bio), Rabbit Anti-NF-κB antibody (1:1000, TA-08, ZSBG-Bio), Anti-iNOS antibody [EPR16635] (1: antibody 1000, ab178945, Abcam, Cambridge, UK) Recombinant Anti-Ym-1 + Ym-2 antibody [EPR15263] (1: Description 10000, ab192029, Abcam), Anti-GAPDH antibody [6C5] -Loading Control (1:10,000, ab8245, Abcam).

Immunofluorescence staining

Dual immunofluorescence staining was used to detect CD86 and CD206 in Iba1-labeled microglia. The green fluorescently labeled Iba1 was the marker of microglia, red fluorescently labeled CD86 was the representative cell surface marker expressed on M1 microglia, while the yellow fluorescently labeled CD206 was the representative cell surface marker expressed on M2 microglia. 2.5×10^4 cells BV-2 cells were inoculated in an 8-well slide with 500 μL/ well, and the cell culture supernatant was discarded after drug administration. The cells on the cell culture slide were fixed with 4% paraformaldehyde (P0099-500ml) at room temperature for 30 min, and then incubated with CD86 (1:200 dilution, AF1447; Beyotime), CD206 (1:200 dilution, 18704-1-AP; Proteintech) and Iba1 (1:200 dilution, ab 283346; Abcam) at 4°C overnight. Subsequently, the cells on the glass slide were rinsed twice with TBS. The cells were incubated with HRP-labeled Goat Anti-Rabbit IgG(H+L) (1:1000 dilution, bs-0295G-HRP, Bioss Antibodies, China) to label CD86 and CD206, and incubated with HRP-labeled Goat Anti-Mouse IgG(H+L) (1:1000 dilution, bs-0296G-HRP; Bioss Antibodies, Beijing, China) to label Iba1 at room temperature for 90 min. After rinsed twice with TBS, Fluoroshield™ containing 4',6-Diamidino-2-phenylindole (DAPI) was used to fix the slides. Finally, the stained cells were observed under a fluorescence microscope (BX43, Olympus) and the fluorescence intensities of CD86, CD206 and Iba1 were analyzed using ImageJ software (National Institutes of Health, Bethesda, MD, USA). Negative controls were performed by omitting the primary antibodies.

Table 1. Experimental grouping and administration.

Groups	Group specification
Control group	Normal control group
SAH group	Model group
SAH+PPF group	Adding the optimal concentration of PPF to treat SAH model cells
SAH+PPF+in-NC group	SAH model construction, PPF treatment + transfection inhibitor negative control
SAH+PPF+in-miR-140-5p group	After constructing *in vitro* SAH model), transfected miR-140-5p mimic
SAH+PPF+OE-NC group	PPF treatment + transfection of blank overexpressed plasmid group
SAH+PPF+OE-TREM-1 group	PPF treatment + transfection of targeted TREM-1 overexpression plasmid
SAH+ mimic-NC group	Transfection mimic-NC after constructing *in vitro* SAH model
SAH+miR-140-5p mimic group	After constructing *in vitro* SAH model), transfected miR-140-5p mimic
SAH+OE-NC group	After *in vitro* SAH model was constructed, OE-NC was transfected
SAH+OE-TREM-1 group	After *in vitro* SAH model was constructed, OE-TREM-1 was transfected
SAH+sh-NC group	After *in vitro* SAH model was constructed, transfected sh-NC
SAH+sh-TREM-1 group	After constructing in vitro SAH model, transfected sh-TREM-1

Luciferase reporter assay

For the dual luciferase reporting experiment, the target gene TREM-1-wild-type (WT-TREM-1) vector and mutant vector (MUT-TREM-1) with miR-140-5p binding sites were designed through an online bioinformatics analysis website. The double luciferase reporter vector plasmid was constructed by Shanghai Shenggong Bioengineering Co. (China). BV-2 cells were transfected with the above vectors and miR-140-5p mimic/mimic-NC for 24 h. The supernatant was collected after cell lysis and centrifugation at 12,000 rpm for 1 min. Then, luciferase activity was detected *via* a dual luciferase detection system.

Statistical analysis

Data were analyzed and mapped using GraphPad Prism 9 (version 9.5.0, La Jolla, CA, USA). Photoshop was used to organize the images. All maps are presented as the means±SDs, and the significant difference between groups was tested by a *t*-test. A *p*-value less than 0.05 was considered significant (**p*<0.05, ***p*<0.01, ****p*<0.001).

Table 2. Primer sequences.

Genes	Primer sequences (5'-3')
miR-140-5p	F:5'-CAGTGGTTTTACCCTATGGTAG-3' R:5'-ACCATAGGGTAAAACCACTGTT-3'
TREM-1	F:5'-TGGTGCCTTGTAGCTGTC-3' R:5'-TCTTTGAAGGCCTCTCTG-3'
iNOS	F:5'-GCTGAACTTGAGCGAGGA-3' R:5'-ACTCAGTGCCAGAAGCTGGA-3'
YM1/2	F:5'-TGGACCTGACTACAATTCCTACA-3' R:5'-AGACCCTGAATACTGCATGGTT-3'
U6	F:5'-GCGCGTCGTGAAGCGTTC -3' R:5'-GTGCAGGGTCCGAGGT-3'
GAPDH	F:5'-ACCACAGTCCATGCCATCAC-3' R:5'-TCACCACCCTGTTGCTGTA -3'

Results

PPF plays a neuroprotective role in SAH by inhibiting neuroinflammation and microglial M1 polarization

After the SAH cell model was constructed with BV-2 cells, the effect of PPF at different concentrations (0, 6.25, 12.5, 25, 50, and 100 μM) on cell viability was determined by CCK-8. Our data revealed that the viability of BV-2 cells in the SAH group was sharply depressed *vs.* the control group ($p<0.001$). The cell viability significantly increased in the 12.5 μM, 25 μM, and 50 μM PPF treatment groups compared to the SAH group ($p<0.001$) (Figure 1A). This suggests that PPF concentrations of 12.5 μM, 25 μM, and 50 μM notably enhanced BV-2 cell viability induced by OxyHb. Among these concentrations, the 25 μM PPF treatment demonstrated the highest viability enhancement. However, no significant changes were observed with 6.25 μM and 100 μM PPF treatments. Consequently, a concentration of 25 μM PPF was chosen for subsequent studies. FCM showed that the apoptosis rate of BV-2 cells in the SAH group was increased by 9.22% *vs.* the control group ($p<0.001$). However, SAH-induced apoptosis was reversed by PPF (Figure 1B). To determine the effect of PPF on SAH-induced neuroinflammation and oxidative damage, we measured the levels of pro-inflammatory factors, ROS production, SOD content, and MDA levels in cells. Our results displayed that SAH induced neuroinflammation by promoting TNF-α, IL-1β, and IL-6 levels in BV-2 cells and induced oxidative damage by increasing ROS production and MDA levels while reducing SOD activity. However, SAH-induced neuroinflammation and oxidative damage could be reversed by PPF (Figure 1 C-F). Subsequently, we further explored the influence of PPF on the polarization of M1 and M2 microglia. RT-qPCR and Western blot results manifested that PPF treatment markedly depressed M1 surface markers (iNOS) and increased M2 surface markers (YM1/2) *vs* the model group

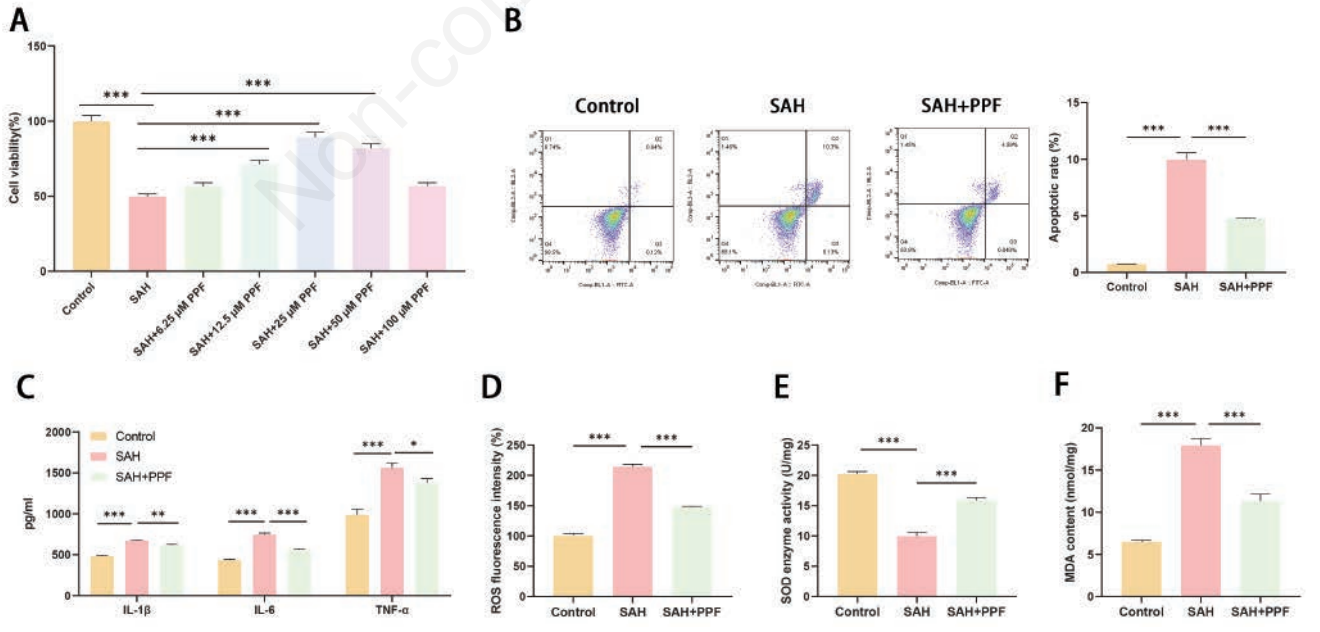

Figure 1. PPF can weaken BV-2 cell damage caused by OxyHb. The SAH cell model was constructed by BV-2 cells, and then PPF administration was performed. **A**) CCK-8 method test of cell proliferation activity. **B**) Flow cytometry detection of apoptosis rate. **C**) The levels of IL-1β, IL-6 and TNF-α in the supernatant of cells were detected by ELISA kit. **D-F**) The oxidative damage of cells was evaluated by SOD, ROS and MDA levels. **p*<0.05, ***p*<0.01, ****p*<0.001, n=3.

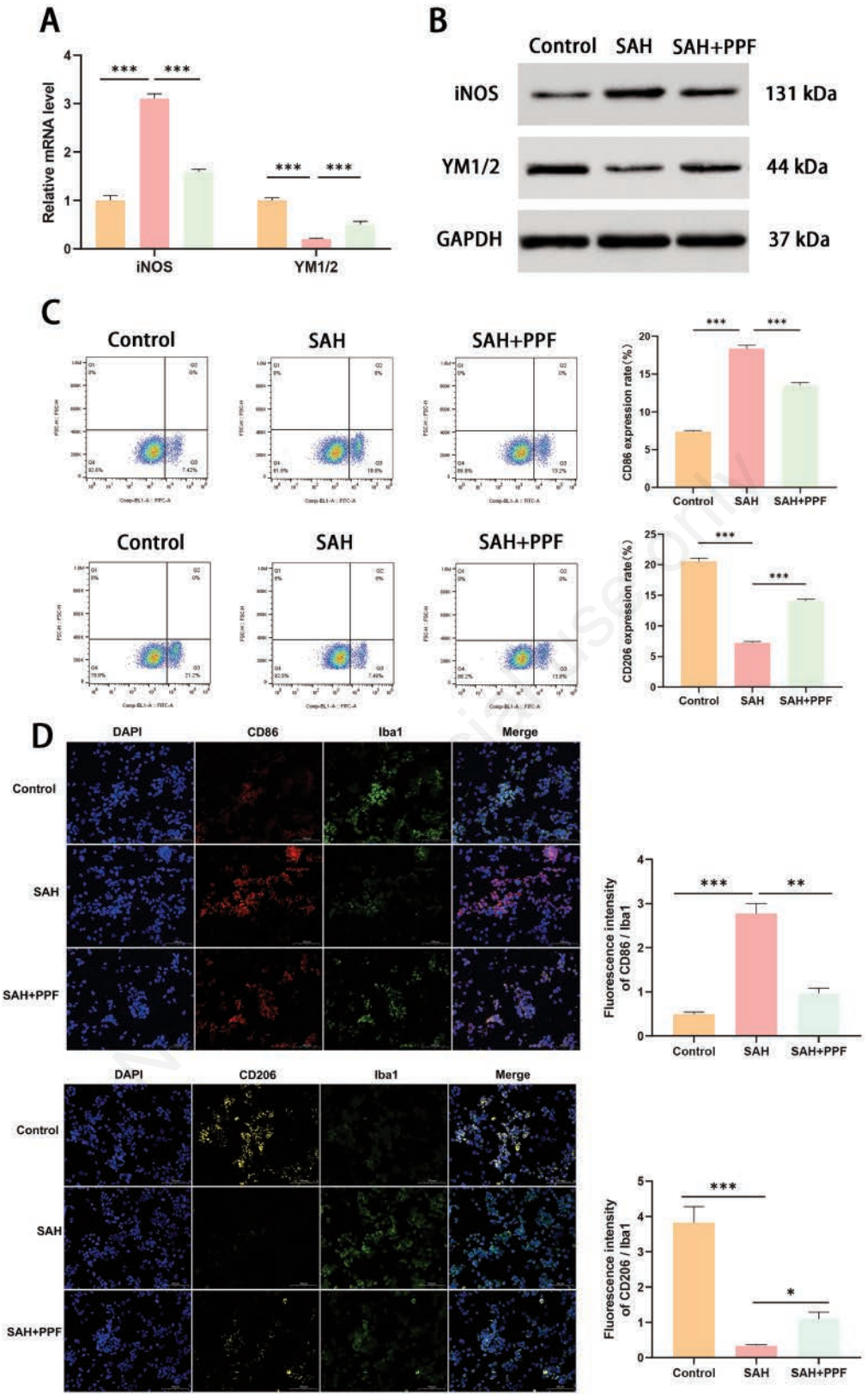

Figure 2. PPF can weaken the M1 polarization of BV-2 cells induced by OxyHb. **A,B**) The expression of M1 surface marker (iNOS) and M2 surface marker (YM1/2) were detected by RT-qPCR and Western blot. **C**) The levels of CD86 (M1 marker) or CD206 (M2 marker) were determined by flow cytometry. **D**) Immunofluorescence detection of CD86 and CD206 in Iba1-labeled microglial cells; scale bars: 100 μm; *p<0.05, **p<0.01, ***p<0.001, n=3.

(p<0.05) (Figure 2 A,B). In addition, the FCM results for CD86 (M1 surface marker) and CD206 (M2 surface marker) revealed that PPF treatment reduced the number of CD86+ microglia and increased the number of CD206+ microglia vs. the model group. By using double immunofluorescence labeling method, we identified that the expression of CD86+ in Iba1-identified microglial cells significantly decreased in the PPF treatment group comparing with model (p<0.01, Figure 2C). On the other hand, CD 206+ in Iba1-identified microglial cell significantly increased comparing with model group (p<0.05, Figure 2D). This evidence suggests that in SAH, PPF can limit microglial M1 polarization and neuroinflammation.

PPF plays a neuroprotective role in SAH by upregulating miR-140-5p

To further explore the specific mechanism of the neuroprotective effect of PPF, detection of miR-140-5p in cells was performed. Our data showed that miR-140-5p was markedly downregulated in the SAH group *vs.* the control group, while PPF upregulated miR-140-5p (p<0.001) (Figure 3A). We then downregulated miR-140-5p in the context of PPF treatment and verified it by RT–qPCR (Figure 3B). Subsequently, biological function experiments showed that downregulation of miR-140-5p reversed the effects of PPF on microglial activity, apoptosis, inflammation and oxidative stress damage (Figure 3 C-H). In addition, RT-qPCR, Western blot, FCM and immunofluorescence staining results showed that the influence of PPF on the polarization of M1 and M2 microglia was reversed after downregulating miR-140-5p (Figure 4 A-D). This evidence strongly confirms that PPF plays a neuroprotective role in SAH by upregulating miR-140-5p.

TREM-1 is involved in the development of SAH as a target gene of miR-140-5p

First, we predicted the binding site of miR-140-5p to TREM-1

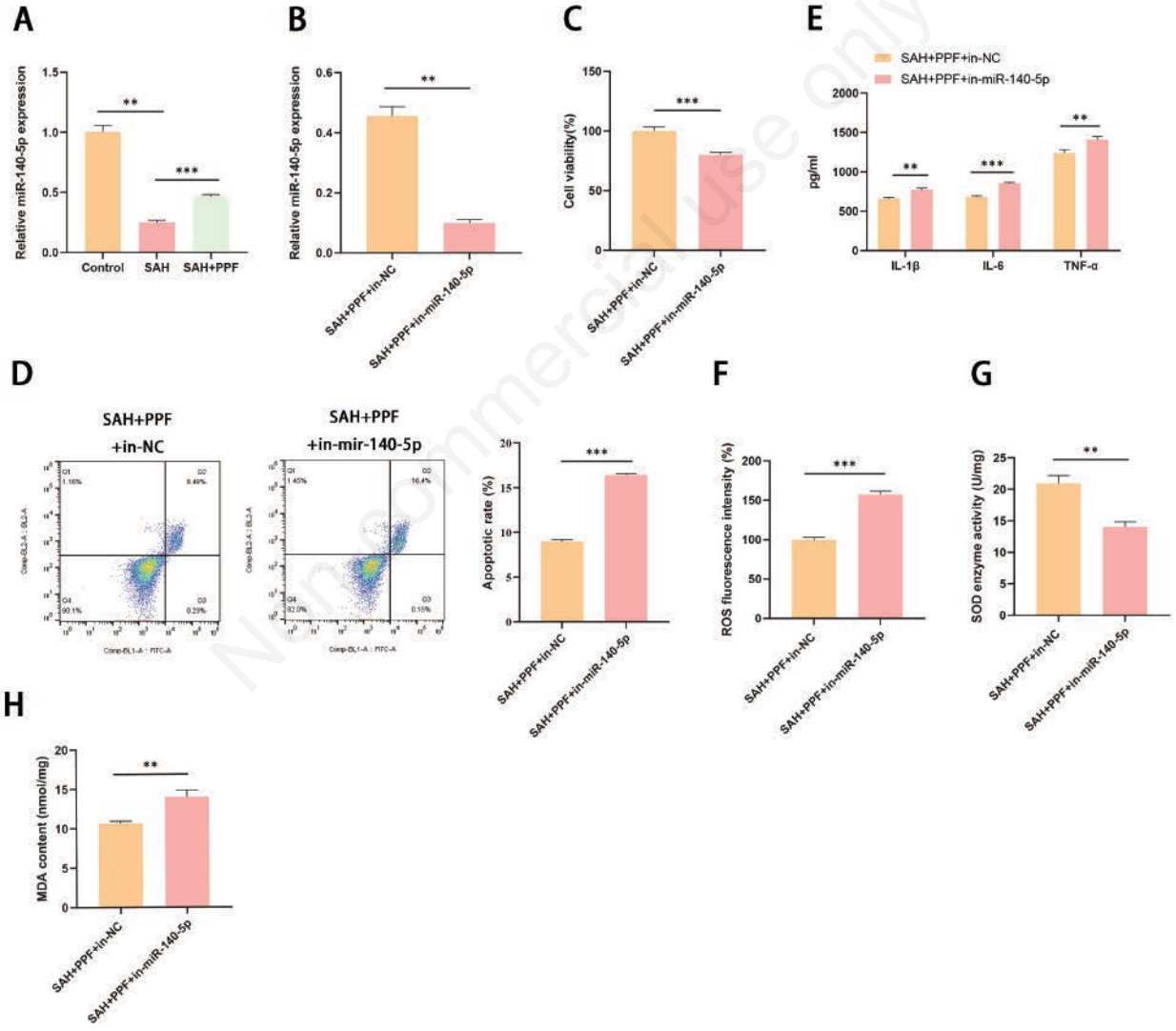

Figure 3. Downregulation of miR-140-5p reversed the ameliorative effect of PPF on SAH cell damage. **A**) RT-qPCR examination of miR-140-5p in cells. **B**) BV-2 cells were transfected with miR-140-5p in the presence of PPF and OxyHb; transfection efficiency of cells. **C**) CCK-8 assay of cell proliferation activity. **D**) Flow cytometry detection of apoptosis rate. **E**) The levels of IL-1β, IL-6 and TNF-α in the supernatant of cells were detected by ELISA kits. **F-H**) The oxidative damage of cells was evaluated by SOD, ROS and MDA levels. **p<0.01, ***p<0.001, n=3.

using a bioinformatics website (Figure 5A). Subsequently, mRNA targeted to miR-140-5p was screened by a dual luciferase reporter assay. As shown in Figure 5B, the luciferase activity decreased after cotransfection of the miR-140-5p mimic with WT-TREM-1 but did not affect the luciferase activity after cotransfection of MUT-TREM-1 with the miR-140-5p mimic. Subsequently, we examined TREM-1 in SAH. As shown in Figure 5C/D, TREM-1 was abnormally highly expressed in SAH, while PPF treatment or overexpression of miR-140-5p reduced TREM-1 levels. Previous studies have shown that activation of the NF-κB signaling cascade is a key downstream target of TREM-1.[20] Subsequently, we silenced or overexpressed TREM-1 in SAH cell models and found that silencing TREM-1 inhibited the activation of the NF-κB signaling cascade, whereas overexpression of TREM-1 had the opposite effect (Figure 5E). In addition, RT–qPCR results showed that silencing TREM-1 significantly reduced the expression of M1 surface markers (iNOS) and increased the expression of M2 surface markers (YM1/2), while overexpression of TREM-1 had the opposite effect (Figure 5F). These data indicate that TREM-1 is the downstream target gene of miR-140-5p and that miR-140-5p inhibits the activation of the NF-κB signaling cascade by targeting TREM-1 expression, thereby inhibiting M1 polarization of SAH microglia.

PPF plays a neuroprotective role in SAH by regulating the miR-140-5p/TREM-1 axis

To further clarify whether PPF affects TREM-1 by regulating the expression of miR-140-5p and thereby participates in the progression of SAH, we conducted a functional salvage experiment. As shown in Figure 6 A,B, the promoting influence of PPF on miR-140-5p could not be affected by overexpression of TREM-1, but the inhibiting influence of PPF on TREM-1 was reversed by

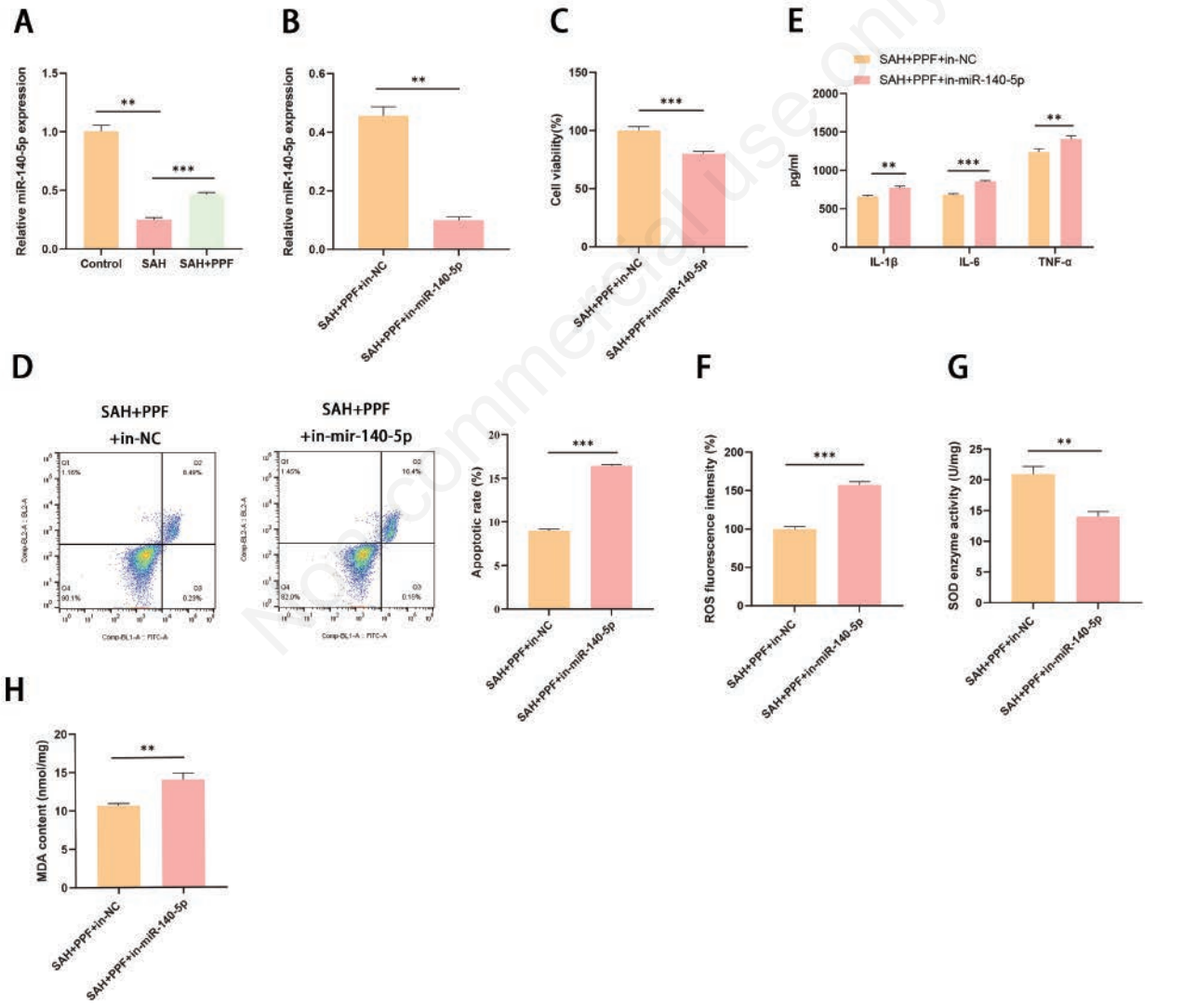

Figure 4. Downregulation of miR-140-5p reversed the effect of PPF on M1/M2 polarization of SAH cells. **A,B**) The expression of M1 surface marker (iNOS) and M2 surface marker (YM1/2) were detected by RT-qPCR and Western blot. **C**) The levels of CD86 (M1 marker) or CD206 (M2 marker) were determined by flow cytometry. **D**) Immunofluorescence detection of CD86 and CD206 in Iba1-labeled microglial cells; scale bars: 100 μm; *p<0.05, **p<0.01, ***p<0.001, n=3.

overexpression of TREM-1 (Figure 6 A,B). The results of biological function experiments showed that after upregulation of TREM-1, the effect of PPF on enhancing cell vitality and inhibiting cell apoptosis, inflammation and oxidative stress damage was weakened (Figure 6 C-H). In addition, RT-qPCR, Western blot, FCM and immunofluorescence staining results showed that the effect of PPF on the polarization of M1 and M2 microglia was reversed after upregulation of TREM-1 (Figure 7 A-D). These results suggest that PPF plays a neuroprotective role in SAH by regulating the miR-140-5p/TREM-1 axis to inhibit M2 polarization and neuroinflammation of microglia.

Discussion

Many studies have verified that microglia play a key role in regulating neuroinflammation in the pathogenesis of EBI after SAH.[21,22] Here, we observed that PPF inhibited oxidative stress damage and pro-inflammatory factor secretion in SAH by regulating the miR-140-5p/TREM-1/NF-κB signaling axis and further promoted the transformation of the microglial M1 phenotype to the M2 phenotype after SAH. To date, this study is the first to investigate the possible molecular mechanism of PPF in microglial inflammation and microglial polarization after SAH.

Previous studies have confirmed that neuroinflammation plays a dominant role in the pathophysiological progression of SAH, including the activation of resident microglia and recruitment of immune cells, as well as the production of large amounts of pro-inflammatory mediators.[22,23] Recent studies have shown that microglia can be polarized into two different phenotypes, M1 (pro-inflammatory) and M2 (anti-inflammatory).[25,26] At the outset of pathological injury in SAH, M1-induced microglial activation is closely related to neuroinflammation through the production of a series of inflammatory mediators, which further leads to neuroinflammation, the immune response, neuronal damage, *etc*.[27-29] Consistent with this theory, our research confirms that SAH-

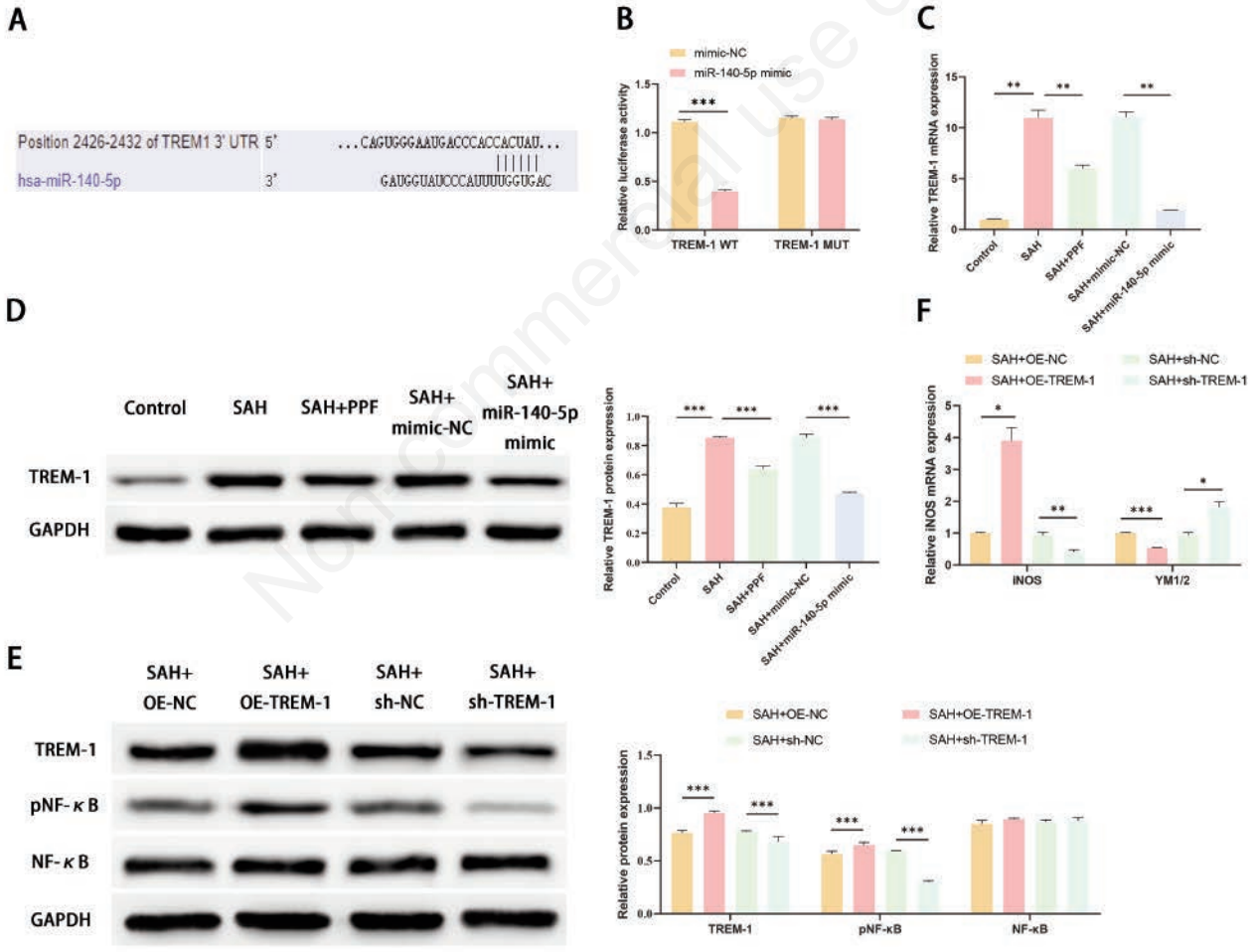

Figure 5. TREM-1 is involved in the development of SAH as a target gene of miR-140-5p. **A**) Prediction of potential binding sites of TREM-1 and miR-140-5p through bioinformatics websites. **B**) Dual luciferase reporting assay evaluation of the interaction of TREM-1 with miR-140-5p. **C,D**) RT-qPCR and Western blot were used to evaluate the effects of PPF treatment or overexpression of miR-140-5p on TREM-1. **E**) shRNA or overexpressed plasmid targeting TREM-1 was transfected into SAH cell models, and the effect of silencing or overexpressing TREM-1 on the NF-κB signaling cascade was evaluated *via* Western blot. F) RT–qPCR examination of iNOS and YM1/2 in cells. *p<0.05, **p<0.01, ***p<0.001, n=3.

induced M1 polarization markers, pro-inflammatory factors and oxidative stress damage were significantly increased, but M1 polarization markers were decreased in microglia.

PPF has been reported to have antioxidant and anti-inflammatory properties and to modulate neuronal apoptosis and immune function properties in a variety of stroke-induced brain injuries.[30-32] Ma *et al*. found that PPF plays a neuroprotective role in stroke by inhibiting inflammatory pathways.[30] In addition, Yu *et al.* found that PPF alleviated inflammatory damage after cerebral infarction by inhibiting the overactivation of microglia.[33] However, the role of PPF in SAH has not been studied. Recent study suggested that PPF exerts anti-inflammatory effects and protects astrocytes from LPS-induced inflammatory injury by downregulating LncRNA-MEG3 expression and inhibiting NF-κB activation. The LncRNA-MEG3/NF-κB axis may represent a potential therapeutic target for PPF's neuroprotective effects.[34] Consistent with this study, we found that PPF can significantly inhibit the release of pro-inflammatory cytokines after SAH while reducing oxidative stress damage. Importantly, our findings suggest that PPF therapy can induce microglia to change from a pro-inflammatory phenotype, M1, to an anti-inflammatory phenotype, M2. In addition, PPF therapy can improve microglial viability and apoptosis, which may be achieved by regulating M2 microglial polarization.

MicroRNAs (miRNAs) are brief, non-coding RNA molecules that modulate gene expression, influencing crucial molecular pathways crucial for tumor growth, resistance to cell death, invasion,

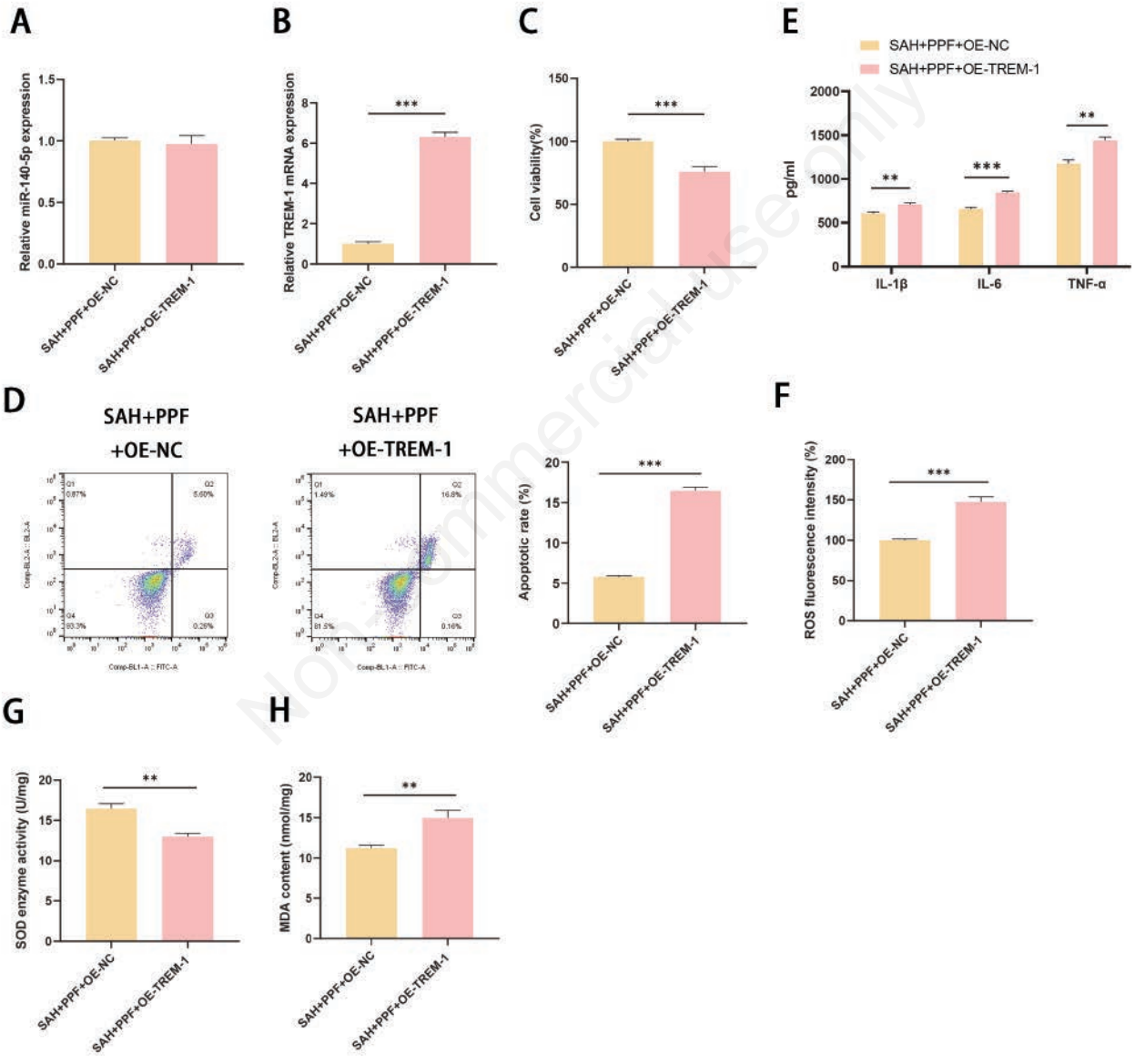

Figure 6. Upregulated TREM-1 reversed the ameliorative effect of PPF on SAH cell damage. With the intervention of PPF and OxyHb, BV-2 cells were transfected with OE-TREM-1. **A,B**) RT-qPCR examination of miR-140-5p and TREM-1 in cells. **C**) The CCK-8 method was used to evaluate the viability of BV-2 cells. **D**) flow cytometry detection of apoptosis rate. **E**) The levels of IL-1β, IL-6 and TNF-α in the supernatant of cells were detected by ELISA kits. F-H) The oxidative damage of cells was evaluated by SOD, ROS and MDA levels. $^{**}p<0.01$, $^{***}p<0.001$, n=3.

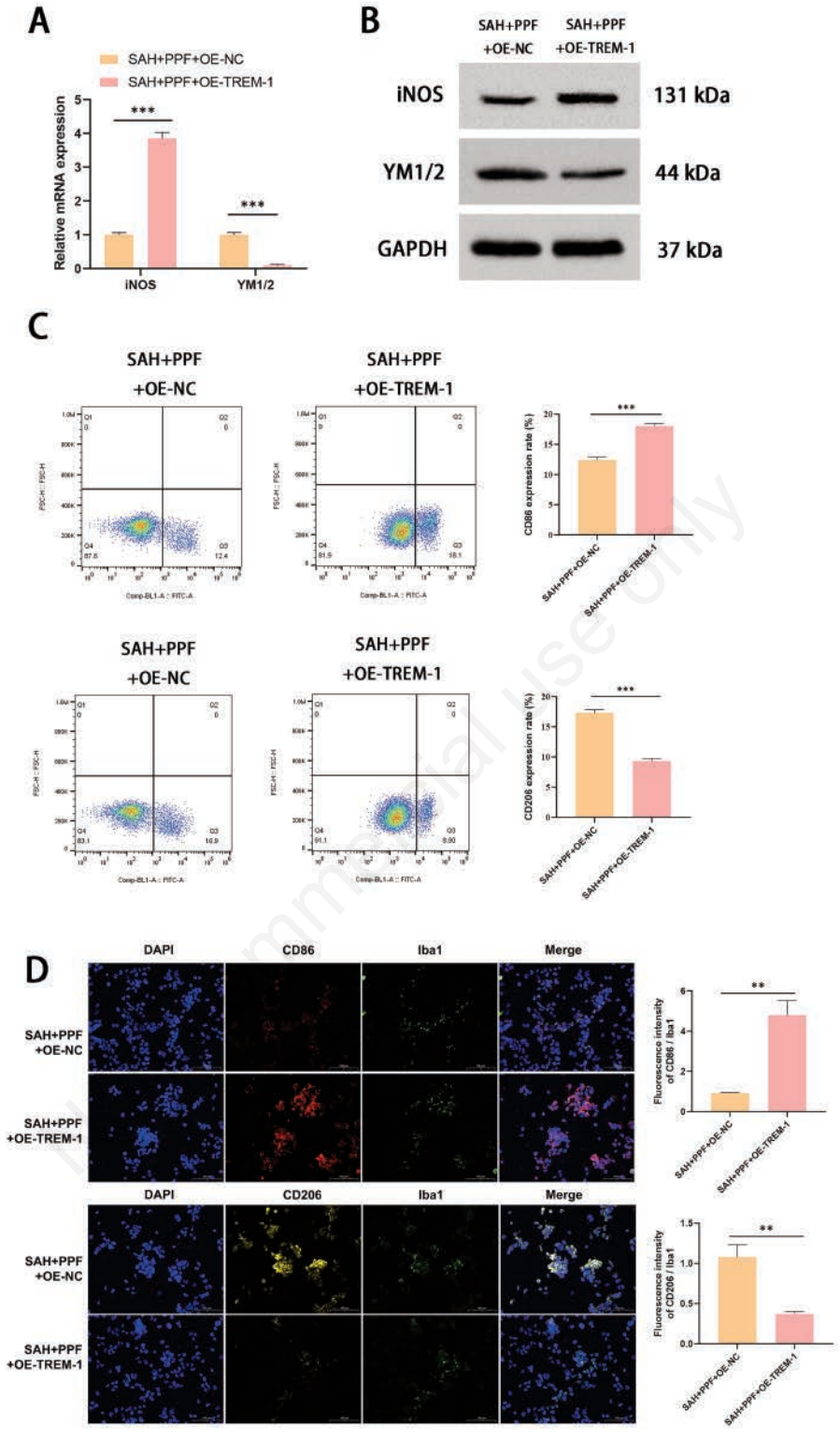

Figure 7. Upregulating TREM-1 reversed the effect of PPF on M1/M2 polarization of SAH cells. **A,B**) The expression of M1 surface marker (iNOS) and M2 surface marker (YM1/2) were detected by RT-qPCR and Western blot. **C**) The levels of CD86 (M1 marker) or CD206 (M2 marker) were determined by flow cytometry. **D**) Immunofluorescence detection of CD86 and CD206 in Iba1-labeled microglial cells; scale bars: 100 μm; $^{**}p<0.01$, $^{***}p<0.001$, n=3.

angiogenesis, and metastasis across various cancer types.[35-39] Dysregulation of miRNA expression in human cancers arises from processes such as miRNA gene amplification or deletion, aberrant transcriptional regulation of miRNAs, disrupted epigenetic modifications, and defects in miRNA biogenesis mechanisms.[30-43] It has been confirmed that miRNAs are highly sensitive to cell stimulation and pathophysiological conditions and directly participate in the adjustment of several key pathophysiological processes after SAH.[44,45] It has been reported that miR-140-5p can reduce SAH-induced microglial activation and the inflammatory response as well as neuronal damage by regulating downstream pathways.[16,17] Importantly, PPF plays a therapeutic role by upregulating miR-140-5p in other diseases.[46] Consistent with previous studies, in this study, we found that miR-140-5p was under expressed in SAH, while PPF treatment significantly promoted miR-140-5p expression. In addition, PPF can inhibit the M1 polarization of microglia and neuroinflammation by upregulating the expression of miR-140-5p, which plays a neuroprotective role in SAH, suggesting that PPF-mediated neuroinflammation may protect against SAH EBI through targeted regulation of miRNA expression and function. miRNA-based disease therapies are in a stage of rapid clinical development,[25] and targeting miR-140-5p may provide innovative and practical therapies for SAH patients.

As an important factor in posttranscriptional gene regulation, miRNAs can participate in disease progression by regulating downstream mRNAs.[47] Here, we found that miR-140-5p targets the 3'-untranslated region of TREM-1, thereby promoting the expression of TREM-1. TREM-1 is a glycoprotein in the immunoglobulin superfamily that plays a key role in innate and adaptive immunity. Sun *et al*. found that TREM-1 was involved in the pathogenesis of SAH-induced EBI.[48] We also noted that TREM-1 can be involved in the activation of the NF-κB signaling cascade by coupling with DAP-12.[20] NF-κB has been shown to play a vital role in inflammatory signaling, bringing about increased expression of pro-inflammatory cytokine genes. More importantly, activation of the NF-κB cascade is related to increased populations of microglia and macrophages in aneurysms.[49] Therefore, in this study, we were interested in the miR-140-5p/TREM-1/NF-κB pathway. Here, we demonstrate that miR-140-5p inhibits NF-κB by targeting TREM-1. From these cumulative studies, we hypothesize that PPF promotes M2 polarization to reduce neuroinflammation after SAH, which may depend on activation of the miR-140-5p/TREM-1/NF-κB signaling axis. As we surmised, TREM-1 is highly expressed in SAH, whereas PPF or overexpression of miR-140-5p can reduce TREM-1 expression. Cell rescue experiments confirmed that overexpressed TREM-1 could reverse the effect of PPF on SAH, suggesting that PPF might play a neuroprotective role in SAH by targeting the miR-140-5p/TREM-1/NF-κB signaling axis.

Overall, our findings provide a novel mechanism by which PPF exerts a neuroprotective role in SAH by targeting the miR-140-5p/TREM-1/NF-κB signaling axis. This has potential implications across various neurological conditions such as stroke, traumatic brain injury, and neurodegenerative diseases, where neuroinflammation and neuronal damage are prominent. However, there are several limitations to this study that warrant consideration. Firstly, our investigation relied on BV-2 cell lines, necessitating validation in an SAH animal model to better simulate the complex *in vivo* environment of SAH. Secondly, while our findings provide valuable insights, potential confounding factors such as variations in cell culture conditions and experimental protocols may influence the robustness and generalizability of our results. Furthermore, the sample size in our study may have restricted the statistical power needed to detect subtle effects. Addressing these limitations is crucial for ensuring the reliability and applicability of our findings to clinical settings. Additionally, the precise mechanisms through which NF-κB modulates the progression of SAH remain incompletely understood and require further investigation to fully elucidate its role. Future investigations could focus on clinical trials to evaluate PPF's efficacy in mitigating conditions like postoperative cognitive dysfunction and sepsis-associated encephalopathy. Mechanistic studies exploring the miR-140-5p/TREM-1 axis could pave the way for novel therapeutic targets and biomarkers, enhancing personalized approaches to neuroprotection in clinical settings.

This study highlights the critical role of PPF in preventing excessive M1 activation of microglia, abnormal release of inflammatory factors, and oxidative damage, which will help ameliorate severe nerve damage after SAH. Importantly, our results suggest that miR-140-5p targeting Trem-1-mediated NF-κB activation is a novel molecular target for the neuroprotective effects of PPF.

References

1. Neifert SN, Chapman EK, Martini ML, Shuman WH, Schupper AJ, Oermann EK, et al. Aneurysmal subarachnoid hemorrhage: the last decade. Transl Stroke Res 2021;12:428-46.
2. Rass V, Helbok R. Early brain injury after poor-grade subarachnoid hemorrhage. Curr Neurol Neurosci 2019;19:78.
3. Leclerc JL, Garcia JM, Diller MA, Carpenter AM, Kamat PK, Hoh BL, et al. A Comparison of pathophysiology in humans and rodent models of subarachnoid hemorrhage. Front Mol Neurosci 2018;11:71.
4. Heinz R, Brandenburg S, Nieminen-Kelha M, Kremenetskaia I, Boehm-Sturm P, Vajkoczy P, et al. Microglia as target for anti-inflammatory approaches to prevent secondary brain injury after subarachnoid hemorrhage (SAH). J Neuroinflamm 2021;18:36.
5. Salter MW, Stevens B. Microglia emerge as central players in brain disease. Nat Med 2017;23:1018-27.
6. Karthikeyan A, Patnala R, Jadhav SP, Eng-Ang L, Dheen ST. MicroRNAs: key players in microglia and astrocyte mediated inflammation in CNS pathologies. Curr Med Chem 2016;23:3528-46.
7. Tsai TH, Chang CH, Lin SH, Su YF, Tsai YC, Yang SF, et al. Therapeutic effect of and mechanisms underlying the effect of miR-195-5p on subarachnoid hemorrhage-induced vasospasm and brain injury in rats. Peerj 2021;9:e11395.
8. Zhou R, Yang Z, Tang X, Tan Y, Wu X, Liu F. Propofol protects against focal cerebral ischemia via inhibition of microglia-mediated proinflammatory cytokines in a rat model of experimental stroke. Plos One 2013;8:e82729.
9. Hou Y, Xiao X, Yu W, Qi S. Propofol suppresses microglia inflammation by targeting TGM2/NF-kappaB signaling. J Immunol Res 2021;2021:4754454.
10. Xiao X, Hou Y, Yu W, Qi S. Propofol ameliorates microglia activation by targeting microRNA-221/222-IRF2 axis. J Immunol Res 2021;2021:3101146.
11. Shi SS, Zhang HB, Wang CH, Yang WZ, Liang RS, Chen Y, et al. Propofol attenuates early brain injury after subarachnoid hemorrhage in rats. J Mol Neurosci 2015;57:538-45.
12. Zhang HB, Tu XK, Chen Q, Shi SS. Propofol reduces inflammatory brain injury after subarachnoid hemorrhage: involvement of PI3K/Akt pathway. J Stroke Cerebrovasc 2019;28:104375.
13. Zheng X, Huang H, Liu J, Li M, Liu M, Luo T. propofol attenuates inflammatory response in LPS-activated microglia by regulating the miR-155/SOCS1 pathway. Inflammation

2018;41:11-9.
14. Wang S, Cui Y, Xu J, Gao H. miR-140-5p attenuates neuroinflammation and brain injury in rats following intracerebral hemorrhage by targeting TLR4. Inflammation 2019;42:1869-77.
15. Song W, Wang T, Shi B, Wu Z, Wang W, Yang Y. Neuroprotective effects of microRNA-140-5p on ischemic stroke in mice via regulation of the TLR4/NF-kappaB axis. Brain Res Bull 2021;168:8-16.
16. Wang P, Dong S, Liu F, Liu A, Wang Z. MicroRNA-140-5p shuttled by microglia-derived extracellular vesicles attenuates subarachnoid hemorrhage-induced microglia activation and inflammatory response via MMD downregulation. Exp Neurol 2023;359:114265.
17. Wang P, Xue Y, Zuo Y, Xue Y, Zhang JH, Duan J, et al. Exosome-encapsulated microRNA-140-5p alleviates neuronal injury following subarachnoid hemorrhage by regulating IGFBP5-mediated PI3K/AKT signaling pathway. Mol Neurobiol 2022;59:7212-28.
18. Sun XG, Ma Q, Jing G, Wang L, Hao XD, Wang GQ. Early elevated levels of soluble triggering receptor expressed on myeloid cells-1 in subarachnoid hemorrhage patients. Neurol Sci 2017;38:873-7.
19. Sun XG, Ma Q, Jing G, Wang GQ, Hao XD, Wang L. Increased levels of soluble triggering receptor expressed on myeloid cells-1 in cerebrospinal fluid of subarachnoid hemorrhage patients. J Clin Neurosci 2017;35:139-43.
20. Sharif O, Knapp S. From expression to signaling: roles of TREM-1 and TREM-2 in innate immunity and bacterial infection. Immunobiology 2008;213:701-13.
21. Pang J, Peng J, Matei N, Yang P, Kuai L, Wu Y, et al. Apolipoprotein E exerts a whole-brain protective property by promoting M1? Microglia quiescence after experimental subarachnoid hemorrhage in mice. Transl Stroke Res 2018;9:654-68.
22. Gao Y, Zhuang Z, Lu Y, Tao T, Zhou Y, Liu G, et al. Curcumin mitigates neuro-inflammation by modulating microglia polarization through inhibiting TLR4 axis signaling pathway following experimental subarachnoid hemorrhage. Front Neurosci 2019;13:1223.
23. Chen J, Zheng ZV, Lu G, Chan WY, Zhang Y, Wong G. Microglia activation, classification and microglia-mediated neuroinflammatory modulators in subarachnoid hemorrhage. Neural Regen Res 2022;17:1404-11.
24. Liu H, Guo D, Wang J, Zhang W, Zhu Z, Zhu K, et al. Aloe-emodin from Sanhua decoction inhibits neuroinflammation by regulating microglia polarization after subarachnoid hemorrhage. J Ethnopharmacol 2024;322:117583.
25. Xia DY, Yuan JL, Jiang XC, Qi M, Lai NS, Wu LY, et al. SIRT1 promotes M2 microglia polarization via reducing ROS-mediated NLRP3 inflammasome signaling after subarachnoid hemorrhage. Front Immunol 2021;12:770744.
26. Tian Y, Liu B, Li Y, Zhang Y, Shao J, Wu P, et al. Activation of RARalpha receptor attenuates neuroinflammation after SAH via promoting M1-to-M2 phenotypic polarization of microglia and regulating Mafb/Msr1/PI3K-Akt/NF-kappaB pathway. Front Immunol 2022;13:839796.
27. Wei J, Li T, Lin S, Zhang B, Li X. Dihydrotestosterone reduces neuroinflammation in spinal cord injury through NF-kappaB and MAPK pathway. Cell Mol Biol 2024;70:213-8.
28. Wu Y, Yang D. Effects of bacterial biofilm on regulation of neurovascular unit functions and neuroinflammation of patients with ischemic cerebral stroke by immunocyte. Cell Mol Biol 2023;69:81-6.
29. Li B, Liang C, Lv Y, Tan Y, Chen W. MiR-22 inhibits myocardial fibrosis in rats with myocardial infarction by targeting PTEN/Akt/mTOR signaling pathway. Cell Mol Biol 2024;70:28-33.
30. Ma Z, Li K, Chen P, Pan J, Li X, Zhao G. Propofol attenuates inflammatory damage via inhibiting NLRP1-Casp1-Casp6 signaling in ischemic brain injury. Biol Pharm Bull 2020;43:1481-9.
31. Yuan J, Cui G, Li W, Zhang X, Wang X, Zheng H, et al. Propofol enhances hemoglobin-induced cytotoxicity in neurons. Anesth Analg 2016;122:1024-30.
32. Wang X, Yang X, Han F, Gao L, Zhou Y. Propofol improves brain injury induced by chronic cerebral hypoperfusion in rats. Food Sci Nutr 2021;9:2801-9.
33. Yu H, Wang X, Kang F, Chen Z, Meng Y, Dai M. Propofol attenuates inflammatory damage on neurons following cerebral infarction by inhibiting excessive activation of microglia. Int J Mol Med 2019;43:452-60.
34. Zhang F, Wang Z, Sun B, Huang Y, Chen C, Hu J, et al. Propofol rescued astrocytes from LPS-induced inflammatory response via blocking LncRNA-MEG3/NF-κB axis. Curr Neurovasc Res 2022;19:5-18.
35. Syed NS, Kamarudin AA, Abdul SS, Norrrahim M, Abdul LN, Wah L. The linkage between microRNA and cancer and its delivery as cancer therapy: a mini-review. Cell Mol Biol 2023;69:7-18.
36. Lai NS, Zhang JQ, Qin FY, Sheng B, Fang XG, Li ZB. Serum microRNAs are non-invasive biomarkers for the presence and progression of subarachnoid haemorrhage. Bioscience Rep 2017;37:BSR20160480.
37. Akdeniz FT, Barut Z. Analysis of miRNA-199-5p expression levels in serum samples of patients with lumbar disc degeneration. Cell Mol Biol 2023;69:83-7.
38. Geng Y, Chen P, Zhang L, Li X, Song C, Wei X et al. LncRNA MALAT1 regulates growth of carcinoma of the lung through modulating miR-338-3p/PYCR2 axis. Cell Mol Biol 2023;69:133-40.
39. Yu K, Xu R, Wu L, Li W, Lin R, Dai M, et al. Effects of microRNA-320 on learning and memory in mice with vascular cognitive impairment caused via cerebral ischemia. Cell Mol Biol 2023;69:112-9.
40. Dai N, Ma H, Feng Y. Silencing of long non-coding RNA SDCBP2-AS1/microRNA-656-3p/CRIM1 axis promotes ferroptosis of lung cancer cells. Cell Mol Biol 2023;69:189-94.
41. Tang Y, Zhang X, Wang S, Liu L, Wang Q, Liu Y, et al. Up-regulation of lncRNA WT1-AS ameliorates Abeta-stimulated neuronal injury through modulation of miR-186-5p/CCND2 axis in Alzheimer's disease. Cell Mol Biol 2024;70:200-6.
42. Bi L, Zhou Y, Zhang Y, Zhang X. MiR-27a-3p exacerbates cell migration and invasion in right-sided/left-sided colorectal cancer by targeting TGFBR2/TCF7L2. Cell Mol Biol 2024;70:148-54.
43. Yu H, Tu S, Shen C, Bai X, Sun J, Shi M, et al. Effects of the lncRNA MALAT1 gene region rs664589 site mutation on acute myocardial infarction in Chinese Han. Cell Mol Biol 2024;70:119-27.
44. Wang WX, Springer JE, Hatton KW. MicroRNAs as biomarkers for predicting complications following aneurysmal subarachnoid hemorrhage. Int J Mol Sci 2021;22:9492.
45. Jafri I. MiRNA a new insight in metabolic and human diseases: a review. Cell Mol Biol 2023;69:102-10.
46. Zhu F, Li Q, Yang Y, Wang L, Wang J. Propofol suppresses proliferation, migration, invasion and promotes apoptosis by upregulating microRNA-140-5p in gastric cancer cells. Oncotargets Ther 2019;12:10129-38.
47. Makowska M, Smolarz B, Romanowicz H. microRNAs in

subarachnoid hemorrhage (review of literature). J Clin Med 2022;11:4630.
48. Sun XG, Duan H, Jing G, Wang G, Hou Y, Zhang M. Inhibition of TREM-1 attenuates early brain injury after subarachnoid hemorrhage via downregulation of p38MAPK/MMP-9 and preservation of ZO-1. Neuroscience 2019;406:369-75.
49. Jin J, Duan J, Du L, Xing W, Peng X, Zhao Q. Inflammation and immune cell abnormalities in intracranial aneurysm subarachnoid hemorrhage (SAH): Relevant signaling pathways and therapeutic strategies. Front Immunol 2022;13:1027756.

Received: 2 April 2024. Accepted: 9 August 2024.

European Journal of Histochemistry 2024; 68:4034
doi:10.4081/ejh.2024.4034